THESIS FOR THE DEGREE OF LICENTIATE OF ENGINEERING

Over the air calibration of transmitter distortion for active antenna arrays

A solution for a non-linearly parametrised model and a general identifiability analysis

Carl Kylin

Department of Electrical Engineering
Chalmers University of Technology
Gothenburg, Sweden, 2024

Over the air calibration of transmitter distortion for active antenna arrays

A solution for a non-linearly parametrised model and a general identifiability analysis

Carl Kylin

Department of Electrical Engineering
Chalmers University of Technology
SE-412 96 Gothenburg, Sweden
Phone: +46 (0)31 772 1000
www.chalmers.se

Cover:
A radar system using the over the air channel to a target of oppurtunity to collect information about the transmitted signal.

Printed by Chalmers Reproservice
Göteborg, Sweden, June 2024

Till Morfar.

Over the air calibration of transmitter distortion for active antenna arrays

A solution for a non-linearly parametrised model and a general identifiability analysis

Carl Kylin
Department of Electrical Engineering
Chalmers University of Technology

Abstract

Radar systems for air surveillance have long utilised large antenna arrays to generate high enough gain for a narrow enough transmitted beam. In most modern systems this is accomplished through the use of large active electronically steered antenna arrays.

Calibrating a large active antenna array is a challenging endeavour. Distorting effects stemming from the amplifying circuitry can have a non-negligible effect on the transmitted signal, and the effects can vary across the array. In modern and future transmitter arrays, individually controlled antenna elements will be a feature. With such systems, distortion that varies over an array can be combatted. One challenge is how to collect data about what signal is being transmitted and in what way the actual signal differs from the desired transmitted signal.

The work presented in this thesis studies aspects of characterising a model describing the distortion generated in an active antenna array using an over the air channel. Specifically, the first included article presents a method where signals collected using an over the air channel generated by targets of opportunity are used to estimate the parameters of a non-linearly parametrised model for a radar transmitter. In this article, the radar is assumed to transmit different signals on each antenna element. The second included article studies conditions for identifiability for the setup in the first article as well as for other similar setups. These works constitute the second part of this thesis.

To put this work into context, the first part of this thesis presents an overview of the problems caused by distortion in a radar system. This is investigated under different modelling assumptions and for radars operating in a number of different modes.

Keywords: Non-linearities, power amplifier, mutual coupling, over the air.

List of Publications

This thesis is based on the following publications:

[A] **Carl Kylin**, Thomas Eriksson, Anders Silander, Tomas McKelvey, "Over-the-air Identification of Coupled Nonlinear Distortion in a MIMO Radar". *Proceedings of the IEEE Sensor Array and Multichannel Signal Processing Workshop*, pp. 121-125, 2022.

[B] **Carl Kylin**, Thomas Eriksson, Anders Silander, Tomas McKelvey, "Identifiability of Models for Nonlinearities in Active Antenna Arrays using Over the Air Measurements". .

Acknowledgments

The work in this thesis would not have been possible without the hundreds of hours of questions, discussions, and feedback from my supervisors. Thank you Thomas, Anders, and Tomas for creating an environment where questions are encouraged, where no-one assumes that they are always correct, and where I am always expected to never do exactly what you say.

Thanks to both Saab and Chalmers for giving me this opportunity to spend so much time doing this work that I so enjoy. Thanks to all my colleagues in both places for taking the time to have a discussion or answer a question.

I want to say thanks to my family for always being there. To my friends for all the good time and for picking me up when I'm feeling down. This journey would have been much more difficult had it not been for your support.

Acronyms

DPD:	Digital predistortion
ILA:	Indirect learning architecture
MIMO:	Multiple-input multiple-output
OTA:	Over the air
PA:	Power amplifier
RADAR (radar):	Radio detection and ranging
RF:	Radio frequency

Contents

Part I

Overview

CHAPTER 1

Introduction

At the advent of twentieth century, Christian Hülsmeyer designed one of the first precursors to what is to today known as a radio detection and ranging system (RADAR, or simply radar) [1]. Hülsmeyer's system, which he called a Telemobiloskop, was envisaged to be used in bad weather to detect the presence of large ships in a specific surveillance volume, e.g., the inlet of a river or a port. Since then, advances in the transmission and reception of electromagnetic radiation at radio frequencies, the introduction of the modern computer and its exponential improvement in processing power, as well as other novel technologies, have significantly altered the architecture and capability of modern radar systems compared to Hülsmeyer's Telemobiloskop. A modern radar system measures a greater number of parameters, providing information about the location, course, and speed of multiple objects in a surveillance volume.

At an overview level, a radar system can be thought of as a computer which probes the surrounding environment through its transmitter and records the response via its receiver. Without a good understanding of the transmitter and receiver, the systems ability to probe the environment will be limited. Accurate models for the transmitter and receiver are therefore important for the radar to perform as well as possible. In a radar, transmission is typically

done at full power, both to increase the transmitted power but also to maximise efficiency. Operating in this area means that power amplifiers (PA) will go into compression and may exhibit strongly non-linear effects. This high power environment is significantly different from that for the receiver, where the environment is best described as highly dynamic, being composed of both strong targets close to, and weak targets far away from, the radar. This thesis sets out to study the problems arising from deviations from the ideal models of the hardware utilised in a radar, specifically those in the transmitter.

To gain an understanding of the potential issues arising from transmitter distortion, one first needs some understanding of the workings of a radar. To this end, Chapter 2 starts of by intoducing models for a pulse-doppler radar transmitting either phased array signals or multiple input multiple output (MIMO) signals. This is followed by a general definition and discussion regarding the sources of distortion in a radar. The type of distortion studied in this work is specified, namely that arising in the transmitter before the antenna array, and the effects of this distortion are investigated for a radar system under different assumptions.

The basic models and high level analysis presented in Chapter 2 highlights the potential issues arising from transmitter distortion and therefore also the gains available from dealing with it. For an operator or manufacturer of radar systems, it can thus act as an initial analysis tool for determining whether or not significant levels of distortion are present in the system. What it does not do is to suggest how to solve the problems. In Chapter 3, methods and publications in literature are presented which tackle various aspects of this problem. Chapter 3 gives an overview of previously published methods, highlighting some open research questions for a radar application and finally the areas of study in this thesis.

This is followed by Chapter 4, where the included papers in this thesis are presented and summarised. Finishing of the first part of this thesis, Chapter 5 concludes and summarises the information presented in previous chapters, as well as presenting potential areas of interest for future research.

CHAPTER 2

Distortion in a radar system

The effects of distortion in a radar system are diverse and depend on both the characteristics of the system as well as the way in which it is operated. In order to understand how the distortion might impact the performance of a radar system, this chapter starts by introducing a simple model for the data collected by a pulsed monostatic radar. This is followed by a brief summary of the type of phenomena that can give rise to any kind of deviation from the ideal model of a radar transmitter. Not all of these phenomena can be described as distortion, some are simply noise. Simple definitions of distortion and noise are declared and used to analyse the impact of transmitter distortion on the information gathered by a radar. The analysis presented in this chapter is meant to give an indication as to how transmitter distortion may impact the performance of a pulsed monostatic radar.

2.1 A crash course in basic radar signal processing

The basic idea of a radar is to transmit an electromagnetic signal towards a collection of objects, typically referred to as targets, and collect information about these from the returning echoes. A modern monostatic pulse-Doppler

radar with an antenna array does this by estimating three parameters: the range, radial velocity, and direction to the target. The range can be inferred from the delay of the returning echo compared to when it was transmitted, the radial velocity from the slight frequency shift of the echo compared to the transmitted signal, and the direction from the orientation of the returning wavefront. To simplify the modelling and estimation of the target parameters, a number of properties are assumed for the signal, target, and radar, such as:

- The transmitted signal is narrowband.
- The target acts as a single point reflector.
- The target is not moving too fast.
- The target is in the far-field of the antenna.
- The antenna spacing is approximately half the wavelength of the carrier-frequency of the signal.

Models under these assumptions are well established, detailed explanations of which can be found in, e.g., [1]. In the following, a simple model for a pulsed monostatic radar is introduced, along with estimation methods and a brief introduction of the detection step. This model is formulated using Kronecker products of steering vectors, which will prove useful when analysing the effect of transmitter distortion.

2.1.1 A pulsed radar signal model

Let $\boldsymbol{X} \in \mathbb{C}^{N_\mathrm{T} \times N_\mathrm{A}}$ be the complex baseband signals transmitted on each antenna element, where N_T are the number transmitted samples per antenna element and N_A are the number of antenna elements. The signal reaching a target in a specific direction will be

$$\boldsymbol{X}\boldsymbol{a}_\mathrm{SS}(\theta, \phi), \tag{2.1}$$

where $\boldsymbol{a}_\mathrm{SS}(\theta, \phi) \in \mathbb{C}^{N_\mathrm{A}}$ is the spatial steering vector, parametrised by the azimuthal angle θ and elevation angle ϕ. The direction is thus specified by the angles θ and ϕ. The entries in the spatial steering vector depend on the antenna geometry. As an example, for a uniform rectangular array with half

wavelength antenna spacing, the spatial steering vector is

$$\begin{aligned}
\boldsymbol{a}_{\mathrm{SS}}(\theta,\phi) &= \boldsymbol{a}_{\mathrm{SS,az}}(\theta) \otimes \boldsymbol{a}_{\mathrm{SS,el}}(\phi), \\
\boldsymbol{a}_{\mathrm{SS,az}}(\theta) &= \begin{bmatrix} 1 & e^{-i\pi\sin(\theta)} & e^{-i2\pi\sin(\theta)} & \cdots e^{-i(N_{\mathrm{A,az}}-1)\sin(\theta)} \end{bmatrix}^T, \\
\boldsymbol{a}_{\mathrm{SS,el}}(\phi) &= \begin{bmatrix} 1 & e^{-i\pi\sin(\phi)} & e^{-i2\pi\sin(\phi)} & \cdots e^{-i(N_{\mathrm{A,az}}-1)\sin(\phi)} \end{bmatrix}^T.
\end{aligned} \tag{2.2}$$

A pulsed radar transmits repetitions of the same pulse in order to aid the estimation of the radial velocity. As long as the target is not moving too fast, the echoes from a single target returning to a single antenna of the radar is approximately

$$\begin{aligned}
\boldsymbol{y} &= \beta \begin{bmatrix} \boldsymbol{S}(\delta)\boldsymbol{X}\boldsymbol{a}_{\mathrm{SS}}(\theta,\phi)\cdot 1 \\ \boldsymbol{S}(\delta)\boldsymbol{X}\boldsymbol{a}_{\mathrm{SS}}(\theta,\phi)\cdot e^{i\omega} \\ \boldsymbol{S}(\delta)\boldsymbol{X}\boldsymbol{a}_{\mathrm{SS}}(\theta,\phi)\cdot e^{i2\omega} \\ \vdots \\ \boldsymbol{S}(\delta)\boldsymbol{X}\boldsymbol{a}_{\mathrm{SS}}(\theta,\phi)\cdot e^{i(N_{\mathrm{P}}-1)\omega} \end{bmatrix} \\
&= \beta\boldsymbol{S}(\delta)\boldsymbol{X}\boldsymbol{a}_{\mathrm{SS}}(\theta,\phi) \otimes \boldsymbol{a}_{\mathrm{ST}}(\omega), \\
\boldsymbol{a}_{\mathrm{ST}}(\omega) &= \begin{bmatrix} 1 & e^{i\omega} & e^{i2\omega} & \vdots & e^{i(N_{\mathrm{P}}-1)\omega} \end{bmatrix}^T,
\end{aligned} \tag{2.3}$$

where $\boldsymbol{y} \in \mathbb{C}^{N_{\mathrm{R}}N_{\mathrm{P}}}$ is the received data, β is the amplitude of the returning echo, $\boldsymbol{S}(\delta) \in \mathbb{C}^{N_{\mathrm{R}}\times N_{\mathrm{R}}}$ is a circular shifting matrix which shifts a vector to the right δ steps, ω is the angular pulse phase rate, N_{P} is the number of pulses, $\boldsymbol{a}_{\mathrm{ST}}(\omega)$ is the slow time steering vector, and $\otimes$ denotes the Kronecker product. For simplicity, this work only considers integer shifts δ. The circular shifting matrix for an integer δ is in this case

$$\begin{aligned}
\boldsymbol{S}(\delta) &= \boldsymbol{S}(1)^{\delta \mod N_{\mathrm{R}}}, \\
\boldsymbol{S}(1) &= \begin{bmatrix} 0 & 0 & 0 & \cdots & 0 & 1 \\ 1 & 0 & 0 & \cdots & 0 & 0 \\ 0 & 1 & 0 & \cdots & \vdots & \vdots \\ \vdots & \ddots & \ddots & \ddots & \vdots & \vdots \\ \vdots & \ddots & \ddots & 1 & 0 & 0 \\ 0 & \cdots & \cdots & 0 & 1 & 0 \end{bmatrix}.
\end{aligned} \tag{2.4}$$

The circularity of this shifting comes from the fact that if the same pulse is transmitted repeatedly it's only possible to estimate the delay δ modulo

the repetition interval, in this case N_R. The astute reader will have noticed that $\boldsymbol{S}(\delta) \in \mathbb{C}^{N_\mathrm{R} \times N_\mathrm{R}}$ and $\boldsymbol{X} \in \mathbb{C}^{N_\mathrm{T} \times N_\mathrm{A}}$, and the product $\boldsymbol{S}(\delta)\boldsymbol{X}$ is therefore well defined only for $N_\mathrm{R} = N_\mathrm{T}$. If $N_\mathrm{R} = N_\mathrm{T}$, the radar is transmitting a pulsed continuous wave signal. If the radar is monostatic and the power of the transmitted signal is high, it may not be possible to receive echoes and transmit simultaneously due to leakage from the transmitter to the receiver. For a monostatic radar, this problem can be solved by alternating between transmission and reception. In this case, the signal model is altered to

$$\boldsymbol{y} = \beta \boldsymbol{S}(\delta) \begin{bmatrix} \boldsymbol{X} \\ \boldsymbol{0}_{(N_\mathrm{R}-N_\mathrm{T}) \times N_\mathrm{A}} \end{bmatrix} \boldsymbol{a}_\mathrm{SS}(\theta, \phi) \otimes \boldsymbol{a}_\mathrm{ST}(\omega), \tag{2.5}$$

where $\boldsymbol{0}_{(N_\mathrm{R}-N_\mathrm{T}) \times N_\mathrm{A}} \in \mathbb{C}^{(N_\mathrm{R}-N_\mathrm{T}) \times N_\mathrm{A}}$ is a matrix full of zeroes. For a monostatic radar with multiple antenna elements the returning signal will travel through the same spatial channel back to the radar as it did leaving and thus be

$$\boldsymbol{y} = \beta \boldsymbol{S}(\delta) \begin{bmatrix} \boldsymbol{X} \\ \boldsymbol{0}_{(N_\mathrm{R}-N_\mathrm{T}) \times N_\mathrm{A}} \end{bmatrix} \boldsymbol{a}_\mathrm{SS}(\theta, \phi) \otimes \boldsymbol{a}_\mathrm{ST}(\omega) \otimes \boldsymbol{a}_\mathrm{SS}(\theta, \phi) + \boldsymbol{w}, \tag{2.6}$$

where $\boldsymbol{y} \in \mathbb{C}^{N_\mathrm{R} N_\mathrm{P} N_\mathrm{A}}$ is the received data consisting of the received data on each antenna element stacked in a single vector, and $\boldsymbol{w}$ is the noise. Although usually presented in another manner, the Kronecker structure is the assumption underlying the typical division of radar data into the three dimensions:

- *Fast time*, along which echoes from a single pulse are arranged.
- *Slow time*, along which the different pulses are arranged.
- *Spatial sampling*, along which the data from each antenna element is arranged.

To illustrate this reordering of the data, suppose one wants to find the data from the 8th sample collected from the 5th pulse on the 13th antenna element. This would be found by setting fast time = 8, slow time = 5, and spatial sampling = 13. This is often presented as a radar data cube, as illustrated in Fig. 2.1.

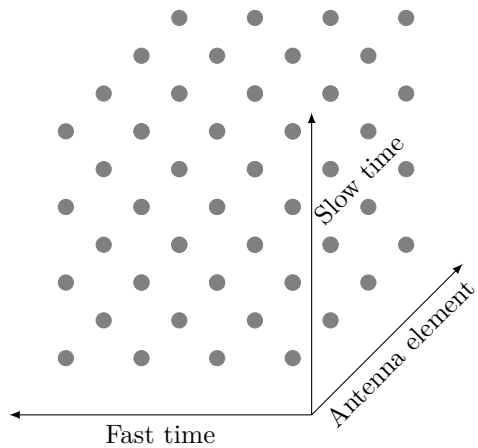

Figure 2.1: The data collected by a radar system is often restructured in three dimensions. Echoes from a single pulse are put in the fast time dimension, the different pulses are arranged in the slow time dimension, and the the data from different antenna elements are arranged along the spatial sampling dimension. This structuring of the data is often referred to as a radar data cube, each point in the cube representing a recorded sample.

For brevity, the model moving forward will be presented as

$$\begin{aligned}
\boldsymbol{y} &= \beta \boldsymbol{a}_{\mathrm{FT}} \otimes \boldsymbol{a}_{\mathrm{ST}} \otimes \boldsymbol{a}_{\mathrm{SS}} + \boldsymbol{w}, \\
\boldsymbol{a}_{\mathrm{FT}} &= \boldsymbol{a}_{\mathrm{FT}}(\delta, \theta, \phi) \\
&= \boldsymbol{S}(\delta) \begin{bmatrix} \boldsymbol{X} \\ \boldsymbol{0}_{(N_{\mathrm{R}} - N_{\mathrm{T}}) \times N_{\mathrm{A}}} \end{bmatrix} \boldsymbol{a}_{\mathrm{SS}}(\theta, \phi), \\
\boldsymbol{a}_{\mathrm{ST}} &= \boldsymbol{a}_{\mathrm{ST}}(\omega), \\
\boldsymbol{a}_{\mathrm{SS}} &= \boldsymbol{a}_{\mathrm{SS}}(\theta, \phi)
\end{aligned} \tag{2.7}$$

2.1.2 Parameter estimation and target detection

To estimate the target parameters $\beta, \delta, \omega, \theta, \phi$, one can use a number of different techniques. A common technique is to utilise the maximum likelihood (ML) estimate. Assuming uncorrelated complex Gaussian noise and a single

target, the ML estimates are given by

$$\hat{\boldsymbol{\theta}} = \begin{bmatrix} \hat{\delta} \\ \hat{\omega} \\ \hat{\theta} \\ \hat{\phi} \end{bmatrix} = \underset{\boldsymbol{\theta}}{\operatorname{argmax}} \frac{\left| \left(\boldsymbol{a}_{\mathrm{FT}} \otimes \boldsymbol{a}_{\mathrm{ST}} \otimes \boldsymbol{a}_{\mathrm{SS}} \right)^H \boldsymbol{y} \right|^2}{\left\| \boldsymbol{a}_{\mathrm{FT}} \otimes \boldsymbol{a}_{\mathrm{ST}} \otimes \boldsymbol{a}_{\mathrm{SS}} \right\|^2}, \tag{2.8}$$

$$\hat{\beta} = \frac{\left(\hat{\boldsymbol{a}}_{\mathrm{FT}} \otimes \hat{\boldsymbol{a}}_{\mathrm{ST}} \otimes \hat{\boldsymbol{a}}_{\mathrm{SS}} \right)^H \boldsymbol{y}}{\left\| \hat{\boldsymbol{a}}_{\mathrm{FT}} \otimes \hat{\boldsymbol{a}}_{\mathrm{ST}} \otimes \hat{\boldsymbol{a}}_{\mathrm{SS}} \right\|^2},$$

where $\cdot^H$ denotes the Hermitian conjugate, $|\cdot|$ denotes absolute value, $\|\cdot\|$ denotes the L2 norm, and $\hat{\boldsymbol{a}}_{\mathrm{FT}}$, $\hat{\boldsymbol{a}}_{\mathrm{ST}}$, $\hat{\boldsymbol{a}}_{\mathrm{SS}}$ are the estimated steering vectors based on the ML estimates $\boldsymbol{\theta} = [\hat{\delta},\ \hat{\omega},\ \hat{\theta},\ \hat{\phi}]$. This type of estimation technique is often called a matched filter, since one attempts to find the best match among a set of available filters. For brevity, the matched filter will be referenced by

$$\mathrm{MF}(\boldsymbol{y}, \boldsymbol{\theta}) = \frac{\left| \left(\boldsymbol{a}_{\mathrm{FT}} \otimes \boldsymbol{a}_{\mathrm{ST}} \otimes \boldsymbol{a}_{\mathrm{SS}} \right)^H \boldsymbol{y} \right|^2}{\left\| \boldsymbol{a}_{\mathrm{FT}} \otimes \boldsymbol{a}_{\mathrm{ST}} \otimes \boldsymbol{a}_{\mathrm{SS}} \right\|^2}. \tag{2.9}$$

In order not to fit the data to noise one can utilise a hypothesis test. This step in the signal processing is called detection, since the presence of a target is detected. Given the parameter estimates, a hypothesis test compares whether it is the possibility that $\boldsymbol{y}$ comes from noise (the null hypothesis $\mathcal{H}_0$) with the possibility that $\boldsymbol{y}$ is distributed according to the estimated distribution (the alternate hypothesis $\mathcal{H}_1$). To determine which hypothesis to choose one can use, e.g., a generalised likelihood ratio test (GLRT). Assuming known noise variance (for the already assumed uncorrelated complex Gaussian noise), the GLRT constitutes

$$\mathrm{MF}(\boldsymbol{y}, \boldsymbol{\theta}) \gtrless_{\mathcal{H}_0}^{\mathcal{H}_1} \gamma, \tag{2.10}$$

i.e., choosing $\mathcal{H}_1$ if the matched filter is greater than γ, and $\mathcal{H}_0$ otherwise. γ is chosen such that the probability of false alarm is less than or equal some desired level.

The modelling, estimation, and detection methods presented here are simple versions of the type of signal processing steps used in a radar. They do not, e.g., take into account unknown noise covariance, the problem of multi-target estimation and detection, any kind of tapering/windowing in slow time or spatial sampling to reduce side-lobes, any other clutter suppression or characterisation techniques, varying radar cross section, nor any way of tackling

extended or very fast targets, to name but a few. They nevertheless describe the main steps used in a radar signal processing chain before detections are passed along to a tracking algorithm, and are deemed sufficiently detailed to facilitate the desired analysis.

2.1.3 The choice of transmitted signal

The model presented so far has made no assumption on the transmitted signal. In the most general case, each transmitting element could transmit an different signal. One choice is to transmit signals that, when time-aligned, are orthogonal, i.e., choosing $\boldsymbol{X}$ such that

$$\boldsymbol{X}^H \boldsymbol{X} = \boldsymbol{I}, \tag{2.11}$$

where $\boldsymbol{I}$ is the identity matrix. If the rank of $\boldsymbol{X}$ is full, the transmitted signal is often called a multiple input multiple output (MIMO) signal. The time-aligned signals do not have to be orthogonal for it to be a MIMO signal, however. If the rank of $\boldsymbol{X}$ is not full, the signal is often called a hybrid MIMO signal. Such a signal choice may originate from the array being divided into sub-arrays or each antenna element transmitting a linear combination of a few orthogonal signals.

Systems transmitting MIMO or hybrid MIMO signals require some degree of individual control over the signal that is transmitted on each antenna element (or sub-array). This requires quite a few digital to analog converting circuits, which can be expensive, bulky, and require high digital data rates. A significantly cheaper option can therefore be to transmit a phased array signal, which only requires a single digital to analog converter and a phase shifter for each antenna element. For a phased array signal, the signal on each antenna element is a phase-altered (and possibly re-scaled) version of the same pulse

$$\boldsymbol{X} = \boldsymbol{x}\boldsymbol{a}_{\mathrm{TX}}^H, \tag{2.12}$$

where $\boldsymbol{a}_{\mathrm{TX}}$ are the transmitter beam-forming weights. By transmitting a phased array signal, the fast time steering vector takes on a slightly simpler form:

$$\boldsymbol{a}_{\mathrm{FT}} = \boldsymbol{S}(\delta) \begin{bmatrix} \boldsymbol{x} \\ \boldsymbol{0}_{(N_{\mathrm{R}}-N_{\mathrm{T}})\times 1} \end{bmatrix} \boldsymbol{a}_{\mathrm{TX}}^H \boldsymbol{a}_{\mathrm{SS}} \tag{2.13}$$

In many radar systems, it is common to use constant amplitude signals, i.e., $|[\boldsymbol{x}]_n| = 1$, where $[\cdot]_n$ denotes the nth entry of the argument vector. For

the phased array setup in this work, this is assumed. For the MIMO and hybrid MIMO models, this is not assumed, primarily because it does not aid later calculations in the same way the constant amplitude assumption does for the phased array. Finally, for later calculations it will be useful to have the response of the matched filter for a phased array to only a target, i.e.,

$$\begin{aligned}\mathrm{MF}(\boldsymbol{y}-\boldsymbol{w},\boldsymbol{\theta}) &= \frac{\left|\left(\boldsymbol{a}_{\mathrm{FT}}\otimes\boldsymbol{a}_{\mathrm{ST}}\otimes\boldsymbol{a}_{\mathrm{SS}}\right)^H(\boldsymbol{y}-\boldsymbol{w})\right|^2}{\left\|\boldsymbol{a}_{\mathrm{FT}}\otimes\boldsymbol{a}_{\mathrm{ST}}\otimes\boldsymbol{a}_{\mathrm{SS}}\right\|^2} \\ &= \frac{\left|\beta\boldsymbol{s}^H\boldsymbol{s}_0\,\boldsymbol{a}_{\mathrm{TX}}^H\boldsymbol{a}_{\mathrm{SS}}\,\boldsymbol{a}_{\mathrm{TX}}^H\boldsymbol{a}_{\mathrm{SS},0}\,\boldsymbol{a}_{\mathrm{ST}}^H\boldsymbol{a}_{\mathrm{ST},0}\,\boldsymbol{a}_{\mathrm{SS}}^H\boldsymbol{a}_{\mathrm{SS},0}\right|^2}{\left\|\boldsymbol{a}_{\mathrm{FT}}\otimes\boldsymbol{a}_{\mathrm{ST}}\otimes\boldsymbol{a}_{\mathrm{SS}}\right\|^2},\end{aligned} \tag{2.14}$$

where the subindex $_0$ to $\boldsymbol{\theta}_0$ and the steering vectors $\boldsymbol{a}_{\dots,0}$ indicate the true parameters and steering vectors. The response of the matched filter for a MIMO signal to only a target is

$$\mathrm{MF}(\boldsymbol{y}-\boldsymbol{w},\boldsymbol{\theta}) = \frac{\left|\beta\boldsymbol{a}_{\mathrm{SS}}^H\begin{bmatrix}\boldsymbol{X}^H & \boldsymbol{0}^H\end{bmatrix}\boldsymbol{S}(\delta)^H\boldsymbol{S}(\delta_0)\begin{bmatrix}\boldsymbol{X}\\ \boldsymbol{0}\end{bmatrix}\boldsymbol{a}_{\mathrm{SS},0}\,\boldsymbol{a}_{\mathrm{ST}}^H\boldsymbol{a}_{\mathrm{ST},0}\,\boldsymbol{a}_{\mathrm{SS}}^H\boldsymbol{a}_{\mathrm{SS},0}\right|^2}{\left\|\boldsymbol{a}_{\mathrm{FT}}\otimes\boldsymbol{a}_{\mathrm{ST}}\otimes\boldsymbol{a}_{\mathrm{SS}}\right\|^2}. \tag{2.15}$$

2.2 Hardware impairments in a radar system

There exist many different forms of hardware impairments that can give rise to problems in a radar system. A non-exhaustive list includes:

- Non-ideal digital to analog and analog to digital conversion.
- Memory effects in circuits due to reflections or non-ideal hardware performance.
- Phase errors over an array due to multiple clocks or a poorly calibrated system.
- Phase noise due to a non-ideal oscillator.
- Thermal noise due to the temperature of circuits.
- Unintended frequency dependent filtering effects of non-ideal circuits.

- Non-linear responses from non-ideal hardware operated under harsh conditions.
- Mutual coupling or leakage between different antenna elements, leading to unintended mixing of the transmitted signals.

The impairments can generally be divided into different categories, depending on what type of issues they cause.

Some, e.g., non-ideal digital to analog and analog to digital conversion, memory effects, unintended filtering, non-linear responses, phase noise, and thermal noise, all act to impair the signal as it travels through a single transmitter or receiver element. Since this impairment happens along the time-axis of the signal, we call these effects temporal impairments. Phase errors over an array and mutual coupling or leakage, on the other hand, act across the antenna elements. We therefore call these effects spatial impairments.

Another way of categorizing the impairments is to consider their reproducibility. Suppose the same signal is transmitted twice under identical conditions. Impairments like non-ideal digital to analog and analog to digital conversion, memory effects, unintended filtering, non-linear responses, phase errors over an array, and mutual coupling or leakage, will generate the same result for both transmissions. In other words they have a deterministic effect on the transmitted signal; with perfect models these effects could be predicted. Such deterministic impairments are called distortion.

Effects such as phase noise and thermal noise, on the other hand, will have a varying effect on the transmitted signal. In other words they are of a stochastic nature. Such stochastic impairments are called noise. That these effects are stochastic does not mean that nothing can be done about them. There are, e.g., ways of tracking the phase noise and thus minimising its impact on the performance of a radar system. Moreover, having an accurate stochastic model of the noise is vital to the performance of signal processing steps. Analysis of methods for tracking the noise and noise modelling mismatch are however beyond the scope of this thesis.

In summary the transmitted signal can be partitioned into three parts:

$$\text{signal} = \text{model} + \text{distortion} + \text{noise}. \tag{2.16}$$

This models the distortion as additive. Given a signal and model vector, it is always possible to decompose the signal into a part parallell with the model

and one orthogonal to it, hence this is quite a general modelling assumption. That being said, for some specific applications, there may be other models that are better suited.

In the following sections, the effects of transmitter temporal distortion are considered. This analysis is initiated by considering identical transmitter temporal distortion from all the transmitter antenna elements and for all pulses. This is extended to more general cases where the transmitter temporal distortion varies from pulse to pulse, or from antenna element to antenna element.

2.3 Identical transmitter distortion for all pulses and antenna elements

Consider a monostatic phased array pulse-Doppler radar modelled according to (2.7) and (2.12). Suppose all antenna elements in the array have identical hardware components operating under identical conditions for all antenna elements and over time, that all phase shifting is ideal and conducted after any distortion, that the array is not effected by any coupling, and that the receiver is ideal.

The type of distortion that may arise in such a system will be temporal from non-ideal hardware components. Because of the above assumptions the distortion will be identical for all pulses and all antenna elements. The distortion will thus be

$$\begin{aligned} \tilde{\boldsymbol{y}} &= \beta \tilde{\boldsymbol{a}}_{\mathrm{FT}} \otimes \boldsymbol{a}_{\mathrm{ST}} \otimes \boldsymbol{a}_{\mathrm{SS}}, \\ \tilde{\boldsymbol{a}}_{\mathrm{FT}} &= \boldsymbol{S}(\delta) \begin{bmatrix} \tilde{\boldsymbol{x}} \\ \boldsymbol{0}_{(N_{\mathrm{R}}-N_{\mathrm{T}})\times 1} \end{bmatrix} \boldsymbol{a}_{\mathrm{TX}}^{H} \boldsymbol{a}_{\mathrm{SS}}(\theta, \phi), \end{aligned} \tag{2.17}$$

where $\tilde{\boldsymbol{y}}$ is the received transmitter distortion, $\tilde{\boldsymbol{a}}_{\mathrm{FT}}$ is the fast time distortion steering vector, and $\tilde{\boldsymbol{x}}$ is the pulse distortion. The transmitter distortion is assumed such that the distortion is zero when nothing is being transmitted. This is not an unreasonable assumption, since if no impulse or power is provided to an electronic system, it will not spontaneously start transmitting something other than thermal noise. To get an idea of the impact of the pulse distortion, suppose the entries of the pulse distortion $\tilde{\boldsymbol{x}}$ are independent zero mean random variables with variance σ_{d}^2. Applying the matched filter to the

received transmitter distortion gives

$$\mathrm{MF}(\tilde{\boldsymbol{y}}, \theta) = \frac{|\beta|^2 \left|\boldsymbol{a}_{\mathrm{FT}}^H \tilde{\boldsymbol{a}}_{\mathrm{FT},0}\right|^2 \left|\boldsymbol{a}_{\mathrm{ST}}^H \boldsymbol{a}_{\mathrm{ST},0}\right|^2 \left|\boldsymbol{a}_{\mathrm{SS}}^H \boldsymbol{a}_{\mathrm{SS},0}\right|^2}{\left\|\boldsymbol{a}_{\mathrm{FT}} \otimes \boldsymbol{a}_{\mathrm{ST}} \otimes \boldsymbol{a}_{\mathrm{SS}}\right\|^2}, \tag{2.18}$$

where $(\boldsymbol{a} \otimes \boldsymbol{b})^H (\boldsymbol{c} \otimes \boldsymbol{d}) = \boldsymbol{a}^H \boldsymbol{c}\, \boldsymbol{b}^H \boldsymbol{d}$ was used. For ease of notation, let

$$\begin{aligned} \tilde{\boldsymbol{s}} &= \boldsymbol{S}(\delta_0) \begin{bmatrix} \tilde{\boldsymbol{x}}^T & \boldsymbol{0}^T \end{bmatrix}^T, \\ \boldsymbol{s} &= \boldsymbol{S}(\delta) \begin{bmatrix} \boldsymbol{x}^T & \boldsymbol{0}^T \end{bmatrix}^T. \end{aligned} \tag{2.19}$$

The only steering vector product affected by distortion will be

$$\boldsymbol{a}_{\mathrm{FT}}^H \tilde{\boldsymbol{a}}_{\mathrm{FT},0} = \left(\boldsymbol{a}_{\mathrm{TX}}^H \boldsymbol{a}_{\mathrm{SS}}\right)^* \boldsymbol{s}^H \tilde{\boldsymbol{s}} \boldsymbol{a}_{\mathrm{TX}}^H \boldsymbol{a}_{\mathrm{SS},0}. \tag{2.20}$$

Since the distortion is assumed zero-mean, and $\boldsymbol{a}_{\mathrm{FT}}^H \tilde{\boldsymbol{a}}_{\mathrm{FT},0}$ is a linear combination of the distortion, it is also zero-mean. To calculate the variance, the property

$$\mathrm{Var}\left[\sum_i \alpha_i z_i\right] = \sum_i \sum_j \alpha_i \alpha_j^* \mathrm{Cov}[z_i, z_j]. \tag{2.21}$$

is needed, where z_i are random variables with finite variance, and α_i are complex coefficients. Using the independence of all samples of the pulse distortion, $|[\boldsymbol{x}]_n| = 1$, and δ, δ_0 being integer, the variance satisfies

$$\mathrm{Var}\left[\boldsymbol{s}^H \tilde{\boldsymbol{s}}\right] = N_{\mathrm{overlap}} \sigma_{\mathrm{d}}^2, \tag{2.22}$$

where

$$N_{\mathrm{overlap}} = \max\left(\left||\delta - \delta_0| - \frac{N_{\mathrm{R}}}{2}\right| - \left(\frac{N_{\mathrm{R}}}{2} - N_{\mathrm{T}}\right), 2N_{\mathrm{T}} - N_{\mathrm{R}}, 0\right) \tag{2.23}$$

are the number of overlapping non-zero samples of $\boldsymbol{s}$ and $\tilde{\boldsymbol{s}}$. If the radar is transmitting a continuous wave signal, then $N_{\mathrm{overlap}} = 2N_{\mathrm{T}} - N_{\mathrm{R}} = N_{\mathrm{R}}$. For a non continuous wave radar, there will be some zeroes in both the vectors $\boldsymbol{s}$ and $\tilde{\boldsymbol{s}}$. The expected value of the distortion in the matched filter is thus

$$\mathbb{E}[\mathrm{MF}(\tilde{\boldsymbol{y}}, \theta)] = \frac{|\beta|^2 N_{\mathrm{overlap}} \sigma_{\mathrm{d}}^2 \left|\boldsymbol{a}_{\mathrm{TX}}^H \boldsymbol{a}_{\mathrm{SS}} \boldsymbol{a}_{\mathrm{TX}}^H \boldsymbol{a}_{\mathrm{SS},0} \boldsymbol{a}_{\mathrm{ST}}^H \boldsymbol{a}_{\mathrm{ST},0} \boldsymbol{a}_{\mathrm{SS}}^H \boldsymbol{a}_{\mathrm{SS},0}\right|^2}{\left\|\boldsymbol{a}_{\mathrm{FT}} \otimes \boldsymbol{a}_{\mathrm{ST}} \otimes \boldsymbol{a}_{\mathrm{SS}}\right\|^2}. \tag{2.24}$$

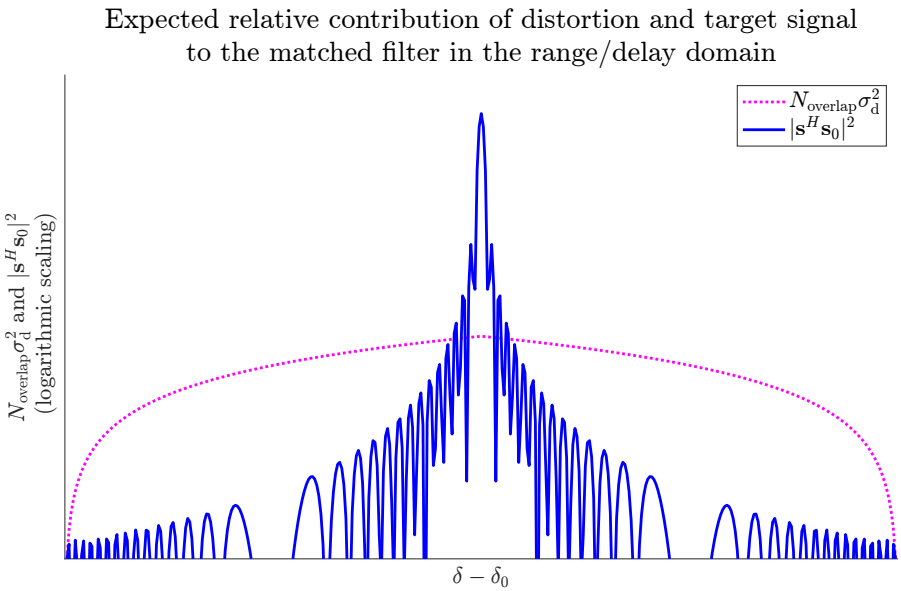

Figure 2.2: Comparison of the relative contribution in the matched filter from the distortion and the target for identical distortion in all pulses and antenna elements in a phased array. The distortion spreads out in the range/delay domain, and is focused in the same way as the target signal in all other domains.

It is not obvious whether this amount of distortion is significant or not. One way of determining this is to compare it with the response from the target from which this distortion is generated from (2.14)

$$\begin{aligned}\frac{\mathbb{E}[\mathrm{MF}(\tilde{\boldsymbol{y}},\boldsymbol{\theta})]}{\mathrm{MF}(\boldsymbol{y}-\boldsymbol{w},\boldsymbol{\theta})} &= \frac{|\beta|^2 N_{\text{overlap}}\sigma_{\text{d}}^2 \left|\boldsymbol{a}_{\text{TX}}^H\boldsymbol{a}_{\text{SS}}\,\boldsymbol{a}_{\text{TX}}^H\boldsymbol{a}_{\text{SS},0}\,\boldsymbol{a}_{\text{ST}}^H\boldsymbol{a}_{\text{ST},0}\,\boldsymbol{a}_{\text{SS}}^H\boldsymbol{a}_{\text{SS},0}\right|^2}{|\beta|^2 \left|\boldsymbol{s}^H\boldsymbol{s}_0\boldsymbol{a}_{\text{TX}}^H\boldsymbol{a}_{\text{SS}}\,\boldsymbol{a}_{\text{TX}}^H\boldsymbol{a}_{\text{SS},0}\,\boldsymbol{a}_{\text{ST}}^H\boldsymbol{a}_{\text{ST},0}\,\boldsymbol{a}_{\text{SS}}^H\boldsymbol{a}_{\text{SS},0}\right|^2} \\ &= \frac{N_{\text{overlap}}\sigma_{\text{d}}^2}{\left|\boldsymbol{s}^H\boldsymbol{s}_0\right|^2}\end{aligned} \tag{2.25}$$

The numerator and denominator are illustrated in Fig. 2.2, for $\sigma_d = 1$ and a non-linearly frequency modulated pulse $\boldsymbol{x}$ of length $N_{\text{T}} = 200$, with $N_{\text{R}} \gg N_{\text{T}}$. The distortion adds power to the side-lobes of the matched filter, potentially masking weaker targets. To deal with strong side-lobes in a system without

distortion, one can utilise multi-target estimation and detection algorithms. Under ideal circumstances, these algorithms can be thought of as removing the target echo and seeing if there were any weaker echoes masked by the side-lobes. Even assuming perfect estimation of a strong target, such methods will not be able to remove the distortion. Although only shown for the parameters $\delta - \delta_0$, the distortion will of course increase the side-lobes for pulse phase rate and direction estimation as well. The relative level of the distortion compared to the target echo is, however, determined by $\delta - \delta_0$.

Increased side-lobes are the main consequence of the this type of distortion. The distortion will also act as an added noise source to all targets, and for targets where the level of distortion is higher or equal the level of the noise, the distortion will have a noticeable negative impact on the accuracy of the estimate. The power of the modelled signal is probably higher than that of the distortion for a realistic system, compared to the equal power assumed here ($|[\boldsymbol{x}]_n| = 1$ and $\sigma_\mathrm{d} = 1$). If so, the impact on the accuracy of the estimate may not be as critical of an issue as the increased side-lobes. A common performance metric for a radar is at what distance it can detect a target with a specific reflection strength. The distortion will be damped equally as much as the modelled signal. Again assuming that power of the modelled signal is higher than that of the distortion, noise will dominate compared to the distortion for a weak echo. The maximum range for detecting a single target may therefore not be so affected by its own distortion. In reality, the weak echo will probably be surrounded by stronger echoes, whose side-lobes will limit the probability of detecting the weak echo.

2.4 Non-identical temporal transmitter distortion

In the previous section, we argued that for a monostatic phased array pulse-Doppler radar under ideal conditions, the transmitter distortion will introduce extra side-lobes, the relative strength of which were solely determined by the delay estimation difference. To reach this conclusion, the definition of distortion was utilised and combined with the following implied symmetry assumptions:

Symmetry 1: The distortion is identical from pulse to pulse.

Symmetry 2: The distortion is identical for different antenna elements.

Any deviation from the above symmetries means that the conclusions from the previous section may no longer be valid. In the following, some radar operational modes and phenomena which might violate these assumptions are exemplified and discussed.

2.4.1 Varying pulse modulation and rapidly changing operating conditions

Transmitting the same pulse repeatedly provides a simple way of probing the radial velocity of a potential target. However, this repetition causes a problem when it comes to identifying the range to a target. If one repeatedly transmits the same pulse towards a target, and then record the generated echo, it will be impossible to determine which pulse generated which echo. This results in an ambiguity in range, only making it possible to estimate the range modulo some maximum range, often called the unambiguous range.

There are many ways to increase the unambiguous range, the most obvious being decreasing the pulse repetition frequency. Another method is to introduce varying pulse modulation, i.e., instead of transmitting the same pulse repeatedly, changing the pulse modulation from one pulse to the next. In this manner each pulse can have a unique signature making it possible to determine the original pulse of a specific echo and therefore estimate the range unambiguously. Beyond solving the range ambiguity problem, this also complicates the task for a repeater jammer. Since the pulse modulation varies from one pulse to the next so will the distortion, therefore violating Sym. 1.

Another way of increasing the unambiguous range of a radar is to transmit pulses at different intervals, either by transmitting one chunk of pulses with one repetition frequency or by constantly varying the pulse repetition interval. After a pulse has been transmitted, the transmitter electronics will be warm and start to cool down until the next pulse is transmitted. If the pulse repetition frequency varies, so will the average temperature of the transmitter circuits, meaning that the distortion in the first chunk of pulses will be different than that in the second. If the time between one pulse to the next constantly varies, so will the temperature. This means that the hardware will have varying operating conditions from one pulse to the next and that the distortion may therefore vary from pulse to pulse. Both of these methods therefore also violate Sym. 1.

A similar problem can occur when a radar is changing its operating con-

ditions quickly over time, e.g., during warm-up or from sudden changes in weather like rain, snow, or wind. Depending on the time scale of these changes, they will violate Sym. 1 to different degrees. Since these effects are transitory, they will be difficult to deal with, but they will also be over after some time, making them less important to combat.

No matter the cause, these effects will introduce distortion which varies from pulse to pulse. This distortion will be

$$\tilde{\boldsymbol{y}} = \beta \boldsymbol{a}_{\mathrm{TX}}^H \boldsymbol{a}_{\mathrm{SS}} \mathrm{vec}\left[\boldsymbol{S}(\delta) \begin{bmatrix} \tilde{\boldsymbol{X}} \\ \boldsymbol{0}_{(N_{\mathrm{R}}-N_{\mathrm{T}})\times N_{\mathrm{P}}} \end{bmatrix}\right] * \boldsymbol{a}_{ST} \otimes \boldsymbol{a}_{\mathrm{SS}}, \tag{2.26}$$

where $*$ is a Khatri-Rao product, vec$[\cdot]$ denotes the vectorisation of the argument matrix, and $\tilde{\boldsymbol{X}} \in \mathbb{C}^{N_{\mathrm{T}}\times N_{\mathrm{P}}}$ is the distortion for each pulse. Again assuming that all pulse distortion entries are independent zero mean random variables with variance σ_{d}^2, applying the phased array matched filter to the received transmitter distortion gives

$$\mathrm{MF}(\tilde{\boldsymbol{y}}, \boldsymbol{\theta}) = \frac{\left|\beta \boldsymbol{a}_{\mathrm{TX}}^H \boldsymbol{a}_{\mathrm{SS}}\, \boldsymbol{a}_{\mathrm{TX}}^H \boldsymbol{a}_{\mathrm{SS},0}\, \boldsymbol{a}_{\mathrm{SS}}^H \boldsymbol{a}_{\mathrm{SS},0}\right|^2 \left|\sum_{p=1}^{N_{\mathrm{P}}} \boldsymbol{s}^H \tilde{\boldsymbol{s}}_p \left[\boldsymbol{a}_{\mathrm{ST}}\right]_p^* \left[\boldsymbol{a}_{\mathrm{ST},0}\right]_p\right|^2}{\left\|\boldsymbol{a}_{\mathrm{FT}} \otimes \boldsymbol{a}_{\mathrm{ST}} \otimes \boldsymbol{a}_{\mathrm{SS}}\right\|^2}, \tag{2.27}$$

where $\tilde{\boldsymbol{s}}_p \in \mathbb{C}^{N_{\mathrm{R}}}$ is defined through

$$\begin{bmatrix} \tilde{\boldsymbol{s}}_1 \\ \tilde{\boldsymbol{s}}_2 \\ \vdots \\ \tilde{\boldsymbol{s}}_{N_{\mathrm{P}}} \end{bmatrix} = \mathrm{vec}\left[\boldsymbol{S}(\delta) \begin{bmatrix} \tilde{\boldsymbol{X}} \\ \boldsymbol{0}_{(N_{\mathrm{R}}-N_{\mathrm{T}})\times N_{\mathrm{P}}} \end{bmatrix}\right] \tag{2.28}$$

Clearly, the effect is no longer limited to the fast time steering vector. The received distortion in the matched filter from each pulse will, similarly to the previous section, have variance

$$\mathrm{Var}\left[\boldsymbol{s}^H \tilde{\boldsymbol{s}}_p\right] = N_{\mathrm{overlap}} \sigma_{\mathrm{d}}^2. \tag{2.29}$$

Using this variance and the fact that $|[\boldsymbol{a}_{\mathrm{ST}}]_p| = |[\boldsymbol{a}_{\mathrm{ST},0}]_p| = 1$,

$$\begin{aligned} \mathrm{Var}\left[\sum_{p=1}^{N_{\mathrm{P}}} \boldsymbol{s}^H \tilde{\boldsymbol{s}}_p \left[\boldsymbol{a}_{\mathrm{ST}}\right]_p^* \left[\boldsymbol{a}_{\mathrm{ST},0}\right]_p\right] &= N_{\mathrm{overlap}} \sigma_{\mathrm{d}}^2 \sum_{p=1}^{N_{\mathrm{P}}} \left|\left[\boldsymbol{a}_{\mathrm{ST}}\right]_p^* \left[\boldsymbol{a}_{\mathrm{ST},0}\right]_p\right|^2 \\ &= N_{\mathrm{P}} N_{\mathrm{overlap}} \sigma_{\mathrm{d}}^2. \end{aligned} \tag{2.30}$$

The expected value of this distortion in the matched filter is

$$\mathbb{E}[\mathrm{MF}(\tilde{\boldsymbol{y}}, \boldsymbol{\theta})] = \frac{|\beta|^2 N_\mathrm{P} N_\mathrm{overlap} \sigma_\mathrm{d}^2 \left|\boldsymbol{a}_\mathrm{TX}^H \boldsymbol{a}_\mathrm{SS} \boldsymbol{a}_\mathrm{TX}^H \boldsymbol{a}_\mathrm{SS,0} \boldsymbol{a}_\mathrm{SS}^H \boldsymbol{a}_\mathrm{SS,0}\right|^2}{\left\|\boldsymbol{a}_\mathrm{FT} \otimes \boldsymbol{a}_\mathrm{ST} \otimes \boldsymbol{a}_\mathrm{SS}\right\|^2}. \tag{2.31}$$

Compared to the filter response from the target:

$$\begin{aligned} \frac{\mathbb{E}[\mathrm{MF}(\tilde{\boldsymbol{y}}, \boldsymbol{\theta})]}{\mathrm{MF}(\boldsymbol{y} - \boldsymbol{w}, \boldsymbol{\theta})} &= \frac{N_\mathrm{P} N_\mathrm{overlap} \sigma_\mathrm{d}^2 \left|\beta \boldsymbol{a}_\mathrm{TX}^H \boldsymbol{a}_\mathrm{SS} \boldsymbol{a}_\mathrm{TX}^H \boldsymbol{a}_\mathrm{SS,0} \boldsymbol{a}_\mathrm{SS}^H \boldsymbol{a}_\mathrm{SS,0}\right|^2}{\left|\beta \boldsymbol{s}^H \boldsymbol{s}_0 \boldsymbol{a}_\mathrm{TX}^H \boldsymbol{a}_\mathrm{SS}\, \boldsymbol{a}_\mathrm{TX}^H \boldsymbol{a}_\mathrm{SS,0}\, \boldsymbol{a}_\mathrm{ST}^H \boldsymbol{a}_\mathrm{ST,0}\, \boldsymbol{a}_\mathrm{SS}^H \boldsymbol{a}_\mathrm{SS,0}\right|^2} \\ &= \frac{N_\mathrm{P} N_\mathrm{overlap} \sigma_\mathrm{d}^2}{\left|\boldsymbol{s}^H \boldsymbol{s}_0 \boldsymbol{a}_\mathrm{ST}^H \boldsymbol{a}_\mathrm{ST,0}\right|^2} = \frac{N_\mathrm{overlap} \sigma_\mathrm{d}^2}{\left|\boldsymbol{s}^H \boldsymbol{s}_0\right|^2} \frac{N_\mathrm{P}}{\left|\boldsymbol{a}_\mathrm{ST}^H \boldsymbol{a}_\mathrm{ST,0}\right|^2}. \end{aligned} \tag{2.32}$$

The comparative contribution of the distortion in the matched filter can thus be factored into the comparative contribution from (2.25) and the factor

$$\frac{N_\mathrm{P}}{\left|\boldsymbol{a}_\mathrm{ST}^H \boldsymbol{a}_\mathrm{ST,0}\right|^2}. \tag{2.33}$$

The numerator and denominator in this fraction are shown in Fig. 2.3. Similarly to Fig. 2.2, the main problem stems from increased side-lobes. This is even more true for this kind of distortion compared to the case in the previous section with identical distortion for all pulses and antenna elements, since the impacts on the estimation error and maximum range of the system are decreased. The comparative contribution of the distortion for small $|\delta - \delta_0|$ and $|\omega - \omega_0|$ is decreased when the distortion varies from pulse to pulse, since the effect of the distortion is 'smeared out' over all $\omega - \omega_0$ instead of being focused in the same manner as a target signal, as was the case in the previous section. This means that the distortion side-lobes are lower for small $|\omega - \omega_0|$, but higher for large $|\omega - \omega_0|$.

2.4.2 Hardware variations, edge environmental effects, antenna amplitude tapering, and multiple input multiple output signals

In the previous section, some phenomena that broke the pulse to pulse distortion symmetry, Sym. 1, were introduced. In a similar fashion this section introduces some phenomena that violate Sym. 2, causing the distortion to vary from one antenna element to the next.

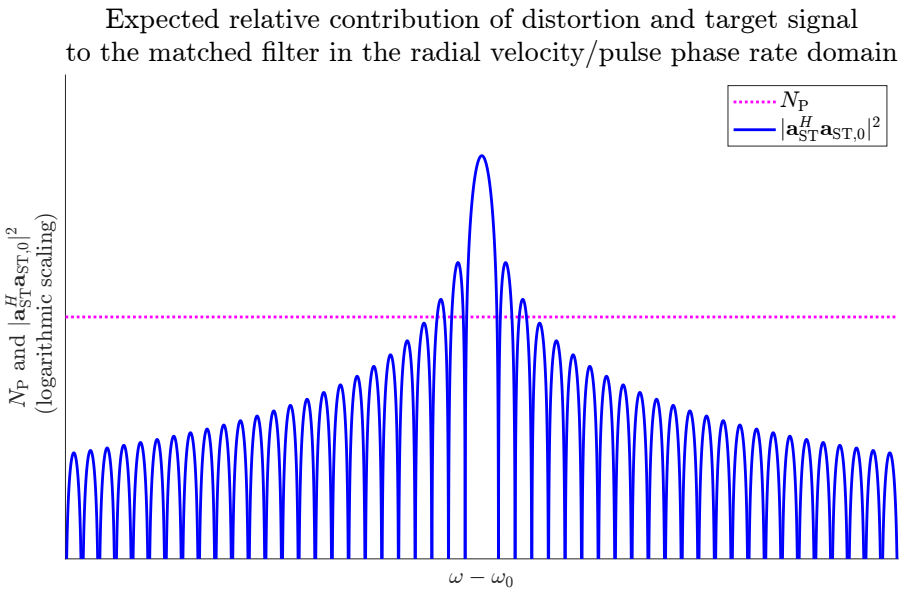

Figure 2.3: Comparison of the relative contribution in the matched filter from the distortion and the target for identical distortion in all antenna elements in a phased array. The distortion spreads out in the range/delay domain as per Fig. 2.2. Because the distortion now varies from one pulse to the next, it will also spread out in the radial velocity/pulse phase rate domain.

Perhaps the most obvious candidate are individual characteristics of components in different antenna elements. The impact of this phenomenon will be limited by manufacturing tolerances for the different components. If the manufacturer manages to produce components with close enough to identical characteristics, then this effect may be negligible.

The transmitter array may experience different temperatures at different elements of the antenna. These temperature variations can appear due to, e.g., cooling differences and load variations across the array.

If a system is subject to any of the above effects, the distortion across the array will no longer be identical, violating Sym. 2, and thus impacting the performance along the antenna element dimension. This type of distortion

will take the form

$$\tilde{\boldsymbol{y}} = \beta \boldsymbol{S}(\delta) \begin{bmatrix} \tilde{\boldsymbol{X}} \\ \boldsymbol{0} \end{bmatrix} \boldsymbol{a}_{\mathrm{SS}} \otimes \boldsymbol{a}_{ST} \otimes \boldsymbol{a}_{\mathrm{SS}}, \tag{2.34}$$

where $\tilde{\boldsymbol{X}} \in \mathbb{C}^{N_{\mathrm{T}} \times N_{\mathrm{A}}}$ is the pulse distortion on each antenna element and the $\boldsymbol{0}$ has dimension $(N_{\mathrm{R}} - N_{\mathrm{T}}) \times N_{\mathrm{A}}$. Yet again assuming that all pulse distortion entries are independent zero mean random variables with variance σ_{d}^2, and applying the phased array matched filter to the received transmitter distortion gives

$$\mathrm{MF}(\tilde{\boldsymbol{y}}, \boldsymbol{\theta}) = \frac{\left|\beta \boldsymbol{a}_{\mathrm{TX}}^H \boldsymbol{a}_{\mathrm{SS}}\, \boldsymbol{a}_{\mathrm{ST}}^H \boldsymbol{a}_{\mathrm{ST},0}\, \boldsymbol{a}_{\mathrm{SS}}^H \boldsymbol{a}_{\mathrm{SS},0}\right|^2 \left|\boldsymbol{s}^H \boldsymbol{S}(\delta_0) \begin{bmatrix} \tilde{\boldsymbol{X}} \\ \boldsymbol{0} \end{bmatrix} \boldsymbol{a}_{\mathrm{SS},0}\right|^2}{\left\|\boldsymbol{a}_{\mathrm{FT}} \otimes \boldsymbol{a}_{\mathrm{ST}} \otimes \boldsymbol{a}_{\mathrm{SS}}\right\|^2}. \tag{2.35}$$

Just as in the two previous sections,

$$\mathrm{Var}\left[\boldsymbol{s}^H \boldsymbol{S}(\delta_0) \begin{bmatrix} \tilde{\boldsymbol{X}} \\ \boldsymbol{0} \end{bmatrix}\right] = N_{\mathrm{overlap}} \sigma_{\mathrm{d}} \boldsymbol{I}, \tag{2.36}$$

where $\boldsymbol{I}$ is the identity matrix.

$$\begin{aligned} \mathrm{Var}\left[\boldsymbol{s}^H \boldsymbol{S}(\delta_0) \begin{bmatrix} \tilde{\boldsymbol{X}} \\ \boldsymbol{0} \end{bmatrix} \boldsymbol{a}_{\mathrm{SS},0}\right] &= N_{\mathrm{overlap}} \sigma_{\mathrm{d}}^2 \left\|\boldsymbol{a}_{\mathrm{SS},0}\right\|^2 \\ &= N_{\mathrm{A}} N_{\mathrm{overlap}} \sigma_{\mathrm{d}}^2 \end{aligned} \tag{2.37}$$

Comparing this with the filter response from the target:

$$\begin{aligned} \frac{\mathbb{E}[\mathrm{MF}(\tilde{\boldsymbol{y}}, \boldsymbol{\theta})]}{\mathrm{MF}(\boldsymbol{y} - \boldsymbol{w}, \boldsymbol{\theta})} &= \frac{N_{\mathrm{A}} N_{\mathrm{overlap}} \sigma_{\mathrm{d}}^2 \left|\beta \boldsymbol{a}_{\mathrm{TX}}^H \boldsymbol{a}_{\mathrm{SS}}\, \boldsymbol{a}_{\mathrm{ST}}^H \boldsymbol{a}_{\mathrm{ST},0}\, \boldsymbol{a}_{\mathrm{SS}}^H \boldsymbol{a}_{\mathrm{SS},0}\right|^2}{\left|\beta \boldsymbol{s}^H \boldsymbol{s}_0\, \boldsymbol{a}_{\mathrm{TX}}^H \boldsymbol{a}_{\mathrm{SS}}\, \boldsymbol{a}_{\mathrm{TX}}^H \boldsymbol{a}_{\mathrm{SS},0}\, \boldsymbol{a}_{\mathrm{ST}}^H \boldsymbol{a}_{\mathrm{ST},0}\, \boldsymbol{a}_{\mathrm{SS}}^H \boldsymbol{a}_{\mathrm{SS},0}\right|^2} \\ &= \frac{N_{\mathrm{A}} N_{\mathrm{overlap}} \sigma_{\mathrm{d}}^2}{\left|\boldsymbol{s}^H \boldsymbol{s}_0\, \boldsymbol{a}_{\mathrm{TX}}^H \boldsymbol{a}_{\mathrm{SS},0}\right|^2} = \frac{N_{\mathrm{overlap}} \sigma_{\mathrm{d}}^2}{\left|\boldsymbol{s}^H \boldsymbol{s}_0\right|^2} \frac{N_{\mathrm{A}}}{\left|\boldsymbol{a}_{\mathrm{TX}}^H \boldsymbol{a}_{\mathrm{SS},0}\right|^2}. \end{aligned} \tag{2.38}$$

Just like in the last section, the comparative contribution of the distortion in the matched filter can be factorised into the comparative contribution from (2.25) and the factor

$$\frac{N_{\mathrm{A}}}{\left|\boldsymbol{a}_{\mathrm{TX}}^H \boldsymbol{a}_{\mathrm{SS},0}\right|^2}, \tag{2.39}$$

which is remarkably similar to the factor (2.33). Since both pulse phase rate and direction estimation essentially boil down to a frequency estimation problem, this is not so surprising. As such, similar conclusions and comments are valid for this result as well. It may be of use to highlight that, while the results in Fig. 2.2 and 2.3 are proportional to the respective dimension of the matched filter, this is not the case for this result. The reception gain $\boldsymbol{a}_{\mathrm{SS}}^H \boldsymbol{a}_{\mathrm{SS},0}$, which cancels out in (2.38), will focus the distortion in the same was as the target. What the fraction (2.39) highlights is that the only way in which the distortion spreads out is through the transmit beam-forming, where the distortion is not focused.

So far this analysis has been limited to a system transmitting a phased array signal. For a MIMO radar, the results of the analysis will differ somewhat. Since a MIMO radar transmits independent signals on each antenna element, the distortion will certainly violate Sym. 2, and will therefore generate similar issues as the hardware variations, edge environmental effects, and antenna amplitude tapering above.

If the all the antenna elements transmit independent signals, then the distortion model in (2.34) is probably quite accurate. Applying the MIMO matched filter to the distortion in (2.34) results in

$$\mathrm{MF}(\tilde{\boldsymbol{y}}, \boldsymbol{\theta}) = \frac{\left|\beta \boldsymbol{a}_{\mathrm{ST}}^H \boldsymbol{a}_{\mathrm{ST},0}\, \boldsymbol{a}_{\mathrm{SS}}^H \boldsymbol{a}_{\mathrm{SS},0}\right|^2 \left|\boldsymbol{a}_{\mathrm{SS}}^H \begin{bmatrix} \boldsymbol{X}^H & \boldsymbol{0}^H \end{bmatrix} \boldsymbol{S}(\delta)^H \boldsymbol{S}(\delta_0) \begin{bmatrix} \tilde{\boldsymbol{X}} \\ \boldsymbol{0} \end{bmatrix} \boldsymbol{a}_{\mathrm{SS},0}\right|^2}{\left\|\boldsymbol{a}_{\mathrm{FT}} \otimes \boldsymbol{a}_{\mathrm{ST}} \otimes \boldsymbol{a}_{\mathrm{SS}}\right\|^2}. \tag{2.40}$$

Comparing this with the MIMO matched filter response to the corresponding target (2.15), gives

$$\frac{\mathbb{E}[\mathrm{MF}(\tilde{\boldsymbol{y}}, \boldsymbol{\theta})]}{\mathrm{MF}(\boldsymbol{y} - \boldsymbol{w}, \boldsymbol{\theta})} = \frac{\mathbb{E}\left[\left|\boldsymbol{a}_{\mathrm{SS}}^H \begin{bmatrix} \boldsymbol{X}^H & \boldsymbol{0}^H \end{bmatrix} \boldsymbol{S}(\delta)^H \boldsymbol{S}(\delta_0) \begin{bmatrix} \tilde{\boldsymbol{X}} \\ \boldsymbol{0} \end{bmatrix} \boldsymbol{a}_{\mathrm{SS},0}\right|^2\right]}{\left|\boldsymbol{a}_{\mathrm{SS}}^H \begin{bmatrix} \boldsymbol{X}^H & \boldsymbol{0}^H \end{bmatrix} \boldsymbol{S}(\delta)^H \boldsymbol{S}(\delta_0) \begin{bmatrix} \boldsymbol{X} \\ \boldsymbol{0} \end{bmatrix} \boldsymbol{a}_{\mathrm{SS},0}\right|^2}, \tag{2.41}$$

where the term $\left|\beta \boldsymbol{a}_{\mathrm{ST}}^H \boldsymbol{a}_{\mathrm{ST},0}\, \boldsymbol{a}_{\mathrm{SS}}^H \boldsymbol{a}_{\mathrm{SS},0}\right|^2$ cancels out. It is difficult to say anything about the expected value in the numerator without very specific assumptions on $\boldsymbol{X}$. The distortion affected the phased array matched filter by

behaving differently compared to the transmitter beam-forming. Since the distortion varies across the array, it is not beam-formed in the same way as the target signal. A MIMO radar will transmit energy in several directions simultaneously. It will therefore not have the same amount of transmit beam-forming gain as the phased array does, and may therefore be more effected by distortion.

2.5 Summary on the effects of transmitter temporal distortion for a modern radar

In this chapter, the effects of transmitter temporal distortion were investigated for pulsed radars operating under different assumptions. Depending on the type of distortion, the way in which the radar system is operated, and the assumptions that can be made about the system, the effects of the distortion can differ greatly. Because the relative strength of the distortion does not depend on the target reflection strength β, the main effects of distortion is the creation of extra side-lobes from strong targets, creating a mask from which it may be difficult to estimate parameters of weaker targets. The ordinary side-lobes created from the signal processing steps used in a radar are possible to suppress using multi-target estimation methods. The side-lobes created by the distortion, however, are usually difficult to remove without either suppressing the distortion at the transmitter or characterising the distortion upon reception. Since the main problem of distortion is to cause higher side-lobe levels, the main benefits of combatting distortion in a radar system is to decrease the side-lobes, lowering the floor of how weak target might be detected. As argued in this chapter, some type of distortion will be more prominent if the radar is operated in a specific way, e.g., using pulse to pulse modulation, MIMO signals, or cheaper hardware with lower manufacturing tolerances. Combatting of distortion may therefore be considered an enabling technology for these types of radar systems.

CHAPTER 3

Linearising a radar system

The purpose of the research presented in this thesis is to study the effects of, and potential remedies to combat, transmitter distortion in a radar. Distortion in radio frequency (RF) transmitters, is by no means a new phenomena, and ample research has been conducted to find models and methods that effectively minimise the effects of distortion in a RF transmitter. This is usually done through lineaisation, a process with the end goal of making the transfer function of the transmitter linear.

In this chapter, first an overview of methods for linearisation of a single power amplifier are presented, describing the move from the first attempts to methods implemented in current RF transmitters. This is followed by an introduction to upcoming challenges in the next generation mutli-antenna transmitter systems. Finally, the research questions investigated in this thesis are presented.

3.1 A brief history of power amplifier linearisation

Katz, Wood, and Chokola present a thorough summary concerning *The Evolution of PA Linearization* in [2], the pertinent points of which are summarised

in this section. In any RF transmitter, the PA plays a crucial role in providing enough signal power to meet performance demands. As output power is increased for a PA, the distorting effects generally increase as well. For any type of physical circuitry there are limits above which they do not function as intended. For a PA, the limit when the output power approaches its maximum possible value, is often referred to as the PA going into compression or saturating. When PAs go into compression, the effects of distortion are much greater compared to when they operate at lower output power levels in a linear region. Why then even choose to operate in this region? One reason is that higher signal power is always good (although perhaps not at the expense of transmitting excessive distortion). The primary reason though, is that "[c]lassical PAs achieve best efficiency at the peak output power, in compression." [2] Considering that the PA is the most power hungry component in most RF transmitters, making sure that the PA efficiency is high is important.

Early attempts at linearisation were carried out by Howard Black in the beginning of the twentieth century, suggesting solutions such as feedforward and feedback linearisation to deal with the effects of distortion.

The solution in use in many communications systems today is either analog or digital predistortion (DPD). Predistortion is based on a simple principle, namely to place an approximate 'pre-inverse' before the PA to counteract the distortion of the PA. In analog predistortion, this is accomplished by placing a predistorter circuit before a PA with approximately inverse characteristic to that PA.

With the move from analog to digital modulation for waveform generation and more efficient but also more non-linear PAs, predistortion moved from analog to DPD. A common technique in the scientific literature is to employ an indirect learning architecture (ILA) solution. In ILA-DPD, a post-inverse is estimated based on the input waveform and measured output of the PA; a model which generates the input waveform from the measured output. This model is then used as the DPD and is fed with the desired output signal. With an ILA-DPD, a model framework is needed for the post-inverse and DPD. Typically, some version of a Volterra series is utilised. For a sampled complex baseband signal $\boldsymbol{x} \in \mathbb{C}^N$, where N is the signal length, a causal

Volterra series takes the form

$$\boldsymbol{y}(n) = \sum_{m=0}^{\infty} \theta_m^1 \boldsymbol{x}(n-m) + \sum_{p=2}^{\infty} \sum_{\substack{m_1 \\ =0}}^{\infty} \sum_{\substack{m_2 \\ =m_1}}^{\infty} \cdots \sum_{\substack{m_p \\ =m_{p-1}}}^{\infty} \sum_{\substack{m_{p+1} \\ =0}}^{\infty} \sum_{\substack{m_{p+2} \\ =m_{p+1}}}^{\infty} \cdots \sum_{\substack{m_{2p-1} \\ =m_{2p-2}}}^{\infty}$$
$$\theta_{m_1,\cdots,m_{2p-1}}^p \prod_{i=1}^{p} \boldsymbol{x}(n-m_i) \prod_{j=p+1}^{2p-1} \boldsymbol{x}^*(n-m_j), \quad (3.1)$$

where $\boldsymbol{y} \in \mathbb{C}^N$ is the sampled output, $\theta_{m_1,\cdots,m_{2p-1}}^p$ are the parameters of the model, and $\cdot^*$ denotes complex conjugate. The Volterra series for a complex baseband signal only contains the specified odd order polynomial terms since all other terms end up outside the complex baseband (at, e.g., frequency $3f_c$, $2f_c$, 0, $-f_c$, $-2f_c$, $-3f_c$, etc., where f_c is the carrier frequency of the transmitted signal). The Volterra series in (3.1) has an infinite number of terms and is therefore only suitable for theoretical studies. Practical implementations of the Volterra series are typically truncated to only include monomials of order $2p-1 \leq P \iff p \leq (P+1)/2$ and memory terms with maximum lag $m_i \leq M$. The number of monomials in a truncated causal baseband Volterra series is

$$\sum_{p=1}^{\frac{P+1}{2}} \left(\!\!\binom{M+1}{p}\!\!\right) \left(\!\!\binom{M+1}{p-1}\!\!\right), \quad (3.2)$$

where

$$\left(\!\!\binom{n}{k}\!\!\right) = \binom{n+k-1}{k} \quad (3.3)$$

is the multiset coefficient, which is equal to the number of ways to choose k from a set of n with replacement disregarding order. This grows very quickly in both M and P. To be able to include higher order terms in terms of both polynomial order and memory lag, some type of model reduction needs to be implemented. There are several model reductions based on the truncated Volterra series, e.g., the memory polynomial [3], the generalised memory polynomial [4], and dynamic deviation reduction [5].

3.2 Power amplifier linearisation in large active antenna arrays

Fager, Eriksson, Barradas, et al., discuss the upcoming challenges of linearising next generation active antenna arrays in the article *New Techniques for Analyzing Efficiency, Linearity, and Linearization in a 5G Active Antenna Transmitter Context* [6]. This section captures the main points of the presented analysis.

In older transmitter systems, especially in a communications setting, the systems have been comprised of a phased array with few antennas, high power per antenna element, serving sectored parts of an environment. In 5G systems, these will "soon be replaced with highly integrated active antenna systems having up to hundreds of individually driven low-power radios operating with very wideband signals."[6] Furthermore, in older communications transmitter systems, mismatch and mutual coupling has been assumed to have a minimal impact on the performance. In cheaper arrays, where components such as isolators or circulators are excluded, and especially for systems transmitting MIMO waveforms, mutual coupling will play a mayor role.

For large antenna arrays experiencing mutual coupling, the balance of power consumption will shift from the PAs and instead be dominated by DPD. This challenge stems from the fact that as the number of antennas grows, the complexity of many DPDs will increase, especially so for a system transmitting MIMO waveforms. Hence, computationally efficient and smart DPD algorithms are needed. Another identified area of interest is how to linearise systems where individual control over each antenna element cannot be assumed, such as a phased array or hybrid MIMO system.

The large antenna arrays predicted to be included in future communications transmitter systems will have a great number of antenna elements. Many modern radar systems already have a great number of antenna elements. Here the transition has more to do with enabling digital sampling of each antenna element in both transmission and reception. In either case, traditional linearisation schemes measure the output after each PA, but in an active antenna array with hundreds of elements (and therefore also PAs), this may not be feasible due to size, power, and cost constraints. Other methods for gathering the data for linearisation are therefore identified as a problem to be solved.

3.3 Linearisation efforts for large active antenna arrays using over the air measurements

The focus of this thesis concerns the effective suppression of distortion in a transmitter of a large active antenna array in a radar context. A solution presented by several authors is to collect data from the antenna array via a number of receivers listening to the transmitted signal via an over the air (OTA) channel. The use of receivers and an OTA channel eliminate the need for sampling the output of each transmitter, reducing hardware complexity. However, as the traditional DPD techniques depend on measuring the output of each antenna element directly, new methods are needed for both characterisation and compensation of distortion in these large antenna arrays.

The choice of model will of course impact the performance and flexibility of the linearisation. A simple model may be very effective under constant conditions, but when conditions change the model parameters may be drastically altered. Still, in systems fulfilling certain simplifying assumptions, simple and lower complexity models may prove very useful. For a phased array, [7], [8] have suggested solutions where the main-beam is sampled and linearised, [9], [10] suggest similar solutions instead sampling one of the side-lobes of the transmitted signal, and finally [11] has suggested a solution assuming all PA have the same model and parameters. For a hybrid MIMO signal, [12] has suggested a solution where the main-beam of each sub-array is estimated and linearised, and [13] suggests a solution assuming all distortion for a sub-array is identical. For systems experiencing only identical temporal distortion (in each sub-array in the case of hybrid MIMO), solutions such as those in [7]–[13] provide low complexity alternatives to otherwise complicated models. For characterising non-identical temporal distortion, however, a model where each PA is considered separately needs to be utilised. For a phased array model, [14] suggests utilising time-division-duplex switches to transmit on one antenna element at a time, effectively turning a phased array transmitter into a time delayed MIMO transmitter, whereas [15], [16] both suggest solutions where data is collected observing the transmission of different signals with several different beam-forming weights. A very similar routine is suggested for a hybrid MIMO setup in [17], i.e., one observing the transmission of many different waveforms over time. For a system transmitting MIMO waveforms, no extra tricks are required as demonstrated by the solution in [18]. Utilising

a more capable model means that the solutions in [14]–[18] can describe the effects of non-identical temporal distortion, providing additional performance compared to the simpler models in [7]–[13]. Even with this added capability, these methods will struggle to handle the effects of mutual coupling. A model which takes into account the combined effects of mutual coupling and temporal distortion caused by PAs and antenna arrays is presented in [19], and is summarised by:

$$\begin{aligned}
\boldsymbol{y}_k(n) = &\sum_{m=0}^{\infty} \alpha_m^{1,k} \boldsymbol{x}_{1,k}(n-m) + \sum_{m=0}^{\infty} \beta_m^{1,k} \boldsymbol{x}_{2,k}(n-m) \\
&+ \sum_{p=2}^{\infty} \sum_{\substack{m_1 \\ =0}}^{\infty} \sum_{\substack{m_2 \\ =m_1}}^{\infty} \cdots \sum_{\substack{m_p \\ =m_{p-1}}}^{\infty} \sum_{\substack{m_{p+1} \\ =0}}^{\infty} \sum_{\substack{m_{p+2} \\ =m_{p+1}}}^{\infty} \cdots \sum_{\substack{m_{2p-1} \\ =m_{2p-2}}}^{\infty} \alpha_{m_1,\cdots,m_{2p-1}}^{p,k} \\
&\qquad \prod_{i=1}^{p} \boldsymbol{x}_{1k}(n-m_i) \prod_{j=p+1}^{2p-1} \boldsymbol{x}_{1,k}^*(n-m_j) \\
&+ \sum_{p=2}^{\infty} \sum_{\substack{m_1 \\ =0}}^{\infty} \sum_{\substack{m_2 \\ =0}}^{\infty} \sum_{\substack{m_3 \\ =m_2}}^{\infty} \cdots \sum_{\substack{m_p \\ =m_{p-1}}}^{\infty} \sum_{\substack{m_{p+1} \\ =0}}^{\infty} \sum_{\substack{m_{p+2} \\ =m_{p+1}}}^{\infty} \cdots \sum_{\substack{m_{2p-1} \\ =m_{2p-2}}}^{\infty} \beta_{m_1,\cdots,m_{2p-1}}^{p,k} \\
&\qquad \boldsymbol{x}_{2,k}(n-m_1) \prod_{i=2}^{p} \boldsymbol{x}_{1,k}(n-m_i) \prod_{j=p+1}^{2p-1} \boldsymbol{x}_{1,k}^*(n-m_j) \\
&+ \sum_{p=2}^{\infty} \sum_{\substack{m_1 \\ =0}}^{\infty} \sum_{\substack{m_2 \\ =0}}^{\infty} \sum_{\substack{m_3 \\ =m_2}}^{\infty} \cdots \sum_{\substack{m_{p+1} \\ =m_p}}^{\infty} \sum_{\substack{m_{p+2} \\ =0}}^{\infty} \sum_{\substack{m_{p+3} \\ =m_{p+2}}}^{\infty} \cdots \sum_{\substack{m_{2p-1} \\ =m_{2p-2}}}^{\infty} \gamma_{m_1,\cdots,m_{2p-1}}^{p,k} \\
&\qquad \boldsymbol{x}_{2,k}^*(n-m_1) \prod_{i=2}^{p+1} \boldsymbol{x}_{1,k}(n-m_i) \prod_{j=p+2}^{2p-1} \boldsymbol{x}_{1,k}^*(n-m_j),
\end{aligned} \tag{3.4}$$

where $\alpha_{m_1,\cdots,m_{2p-1}}^{p,k}$, $\beta_{m_1,\cdots,m_{2p-1}}^{p,k}$, and $\gamma_{m_1,\cdots,m_{2p-1}}^{p,k}$ Are the parameters of the model, $\boldsymbol{x}_{1,k} \in \mathbb{C}^N$ is the input to and $\boldsymbol{y}_k \in \mathbb{C}^N$ the output of the PA of element k in the array, and $\boldsymbol{x}_{2,k} \in \mathbb{C}^N$ is the coupling signal for element k, defined by

$$\boldsymbol{x}_{2,k}(n) = \sum_{l \neq k} \sum_{m=0}^{\infty} \lambda_{k,l,m} \boldsymbol{y}_l(n-m), \tag{3.5}$$

where $\lambda_{k,l,m}$ are the mutual coupling coefficients. The model in [19] includes truncations on the polynomial order and maximum memory lag included in

(3.4) for the different type of terms (α, β, γ), as well as a truncation on the memory in (3.5). The mutual coupling coefficients $\lambda_{k,l,m}$ are assumed known, either from simulations of the antenna array or through separate measurements of the array.

This model is used in an OTA setting in [20], [21]. In an OTA setting this model is no longer linearly parametrised by the parameters $\alpha^{p,k}_{m_1,\cdots,m_{2p-1}}$, $\beta^{p,k}_{m_1,\cdots,m_{2p-1}}$, and $\gamma^{p,k}_{m_1,\cdots,m_{2p-1}}$ because of the unknown coupling signal $\boldsymbol{x}_{2,k}$. This additional complication is dealt with in [20] by making some linearising simplifications. In [21], the authors suggest an iterative least squares minimisation routine with a few linear approximations.

All the sources above deal with a setup relevant for a communications setup where a few receivers are used to gather information about the transmitted signal. A monostatic radar system already has receivers built into the system, hence an interesting application may be to utilise this resource for OTA calibration. While the model in (3.4) and (3.5) is certainly non-linearly parametrised, it still has some structure providing information that can be utilised. This is the area under investigation in Paper A, where a known OTA channel for a MIMO radar is assumed and the parameter estimation is instead carried out via a non-linear optimisation routine.

While conducting the work published in Paper A, non-apparent phenomena influencing the performance of the parameter estimation was observed. From a big picture perspective, it is relatively obvious that the more receivers that are used in an OTA setting, the more information is collected. But how many receivers are needed and how does this relate to the number of antenna elements in the array and type of transmitted signal? This is the area under investigation in Paper B, where a general model for different transmitted signals is combined with a versatile OTA channel description to study what the limiting requirements are on the problem.

CHAPTER 4

Summary of included papers

This chapter provides a summary of the included papers.

4.1 Paper A

Carl Kylin, Thomas Eriksson, Anders Silander, Tomas McKelvey
Over-the-air Identification of Coupled Nonlinear Distortion in a MIMO Radar
Published in
Proceedings of the IEEE Sensor Array and Multichannel Signal Processing Workshop,
pp. 121–125, Trondheim, Norway, 2022
 DOI: 10.1109/SAM53842.2022.9827893.

This conference contribution presents a method for estimating the parameters of a transmitter array under the effects of coupled non-linear distortion. The output of the array, modelled by a non-linearly parametrised model, is measured over a known over the air channel. Since the output is not linearly dependent on the model parameters, estimating the parameters is a non-trivial

task. In this contribution, derivatives of the output of the transmitter array w.r.t. the model parameters are derived. These derivatives are then used in a Gauss-Newton type estimation algorithm, which is demonstrated on simulated data.

4.2 Paper B

Carl Kylin, Thomas Eriksson, Anders Silander, Tomas McKelvey
Identifiability of Models for Nonlinearities in Active Antenna Arrays using Over the Air Measurements
.

This article presents a general framework for modelling different types of transmitter arrays, ranging from phased array to hybrid and full multiple input multiple output transmitter arrays. This transmitter model is joined with an assumed known over the air channel, and identifiability requirements are investigated for different transmitter arrays using different over the air channels. The initial identifiability analysis concerns a linearly parametrised model. The analysis is subsequently extended to cover a non-linearly parametrised model, highlighting the differing results. Finally, a short discussion regarding the application of the derived requirements is presented.

CHAPTER 5

Concluding Remarks and Future Work

Depending on the type of radar that is utilised and in what way it is used, the effects of distortion may vary greatly. For a monostatic pulsed phased array radar operating under ideal assumptions, the relative contribution of distortion is determined by the difference in range/delay. The main problem arising from this distortion were higher side-lobes that are difficult to impossible to suppress without doing something about the distortion. For radar systems operating under less stringent assumptions or according to another scheme, the effects were no longer solely determined by the difference in range/delay. Still, the main effects were similar, namely to mask weaker targets in proximity to stronger targets.

Historically, different methods have been utilised to linearise different systems. One of the more popular methods today for RF transmitters is based on employing an approximate 'pre-inverse' before the system to predistort the input to the system. This method relies on a model for the pre-inverse, the parameters of which are estimated based on the input and measured output of each antenna element in the transmitter. For large antenna arrays in future transmitter systems, this thesis has highlighted two challenges: they may be more sensitive to mutual coupling between elements and it may no longer be

feasible to conduct indvidual measurements of the output of each antenna element in the array. A model structure that can capture the effects of mutual coupling was introduced to deal with the first problem. To deal with the second problem, one possible solution is to utilise an OTA channel.

It is with this background that the contributions presented in this thesis should be viewed. Previous publications have suggested different models to deal with this issue. The first contribution included in this thesis presents a solution to the problem of estimating the parameters of the mutual coupling model using a known OTA channel. The second contribution included in this thesis contains an analysis regarding the identifiability of models for different types of transmitter systems using different types of known OTA channels.

In future works it would be interesting to present a solution to the blind calibration issue, i.e., joint estimation of the transmitter parameters and the channel parameters. Other radar specific applications of linearisation may also be of interest, e.g., linearisation of radar specific waveforms and investigations into what type of linearisation procedure is most suited for a radar.

References

[1] M. A. Richards, *Fundamentals of radar signal processing [electronic resource]*. McGraw-Hill Education LLC., 2014, ISBN: 0071798323.

[2] A. Katz, J. Wood, and D. Chokola, "The evolution of PA linearization, From classic feedforward and feedback through analog and digital predistortion," *IEEE Micorwave Magazine*, vol. 17, no. 2, pp. 32–40, Jan. 2016. DOI: 10.1109/MMM.2015.2498079.

[3] J. Kim and K. Konstantinou, "Digital predistortion of wideband signals based on power amplifier model with memory," *Electronics Letters*, vol. 37, no. 23, pp. 1417–1418, Nov. 2001, ISSN: 00135194. DOI: 10.1049/el:20010940.

[4] D. R. Morgan, Z. Ma, J. Kim, M. G. Zierdt, and J. Pastalan, "A generalized memory polynomial model for digital predistortion of RF power amplifiers," *IEEE Transactions on Signal Processing*, vol. 54, no. 10, pp. 3852–3860, Oct. 2006, ISSN: 1053587X. DOI: 10.1109/TSP.2006.879264.

[5] A. Zhu, P. J. Draxler, J. J. Yan, T. J. Brazil, D. F. Kimball, and P. M. Asbeck, "Open-loop digital predistorter for RF power amplifiers using dynamic deviation reduction-based volterra series," *IEEE Transactions on Microwave Theory and Techniques*, vol. 56, no. 7, pp. 1524–1534, Jun. 2008, ISSN: 00189480. DOI: 10.1109/TMTT.2008.925211.

[6] C. Fager, T. Eriksson, F. Barrradas, K. Hausmair, T. Cunha, and J. C. Pedro, "Linearity and efficiency in 5g transmitters, New techniques for

analyzing efficiency, linearity, and linearization in a 5g active antenna transmitter context," *IEEE Microwave Magazine*, vol. 20, no. 5, pp. 35–49, Apr. 2019. DOI: 10.1109/MMM.2019.2898020.

[7] F. Jalili, F. F. Tafuri, O. K. Jensen, Y. Li, M. Shen, and G. F. Pedersen, "Linearization trade-offs in a 5G mmwave active phased array OTA setup," *IEEE Access*, vol. 8, pp. 110 669–110 677, 2020, ISSN: 21693536. DOI: 10.1109/ACCESS.2020.3002348.

[8] A. Brihuega, M. Abdelaziz, M. Turunen, T. Eriksson, L. Anttila, and M. Valkama, "Linearizing active antenna arrays: Digital predistortion method and measurements," in *2019 IEEE MTT-S International Microwave Conference on Hardware and Systems for 5G and Beyond, IMC-5G 2019*, Aug. 2019, ISBN: 9781728131436. DOI: 10.1109/IMC-5G47857.2019.9160379.

[9] A. B. Ayed, G. Scarlato, P. Mitran, and S. Boumaiza, "On the effectiveness of near-field feedback for digital pre-distortion of millimeter-wave RF beamforming arrays," *IEEE MTT-S International Microwave Symposium Digest*, vol. 2020-August, pp. 547–550, Aug. 2020, ISSN: 0149645X. DOI: 10.1109/IMS30576.2020.9223791.

[10] Q. Luo, X. W. Zhu, C. Yu, *et al.*, "Linearization angle widened digital predistortion for 5G MIMO beamforming transmitters," *IEEE Transactions on Microwave Theory and Techniques*, vol. 69, no. 11, pp. 5008–5020, Nov. 2021, ISSN: 15579670. DOI: 10.1109/TMTT.2021.3098600.

[11] W. Pan, C. Li, X. Quan, *et al.*, "Digital linearization of multiple power amplifiers in phased arrays for 5G wireless communications," in *2018 IEEE International Symposium on Signal Processing and Information Technology, ISSPIT 2018*, IEEE, Feb. 2019, pp. 247–251, ISBN: 9781538675687. DOI: 10.1109/ISSPIT.2018.8642775.

[12] X. Liu, W. Chen, L. Chen, F. M. Ghannouchi, and Z. Feng, "Linearization for hybrid beamforming array utilizing embedded over-the-air diversity feedbacks," *IEEE Transactions on Microwave Theory and Techniques*, vol. 67, no. 12, pp. 5235–5248, Dec. 2019, ISSN: 15579670. DOI: 10.1109/TMTT.2019.2944821.

[13] A. Brihuega, L. Anttila, M. Abdelaziz, T. Eriksson, F. Tufvesson, and M. Valkama, "Digital predistortion for multiuser hybrid MIMO at mmwaves," *IEEE Transactions on Signal Processing*, vol. 68, pp. 3603–3618, 2020, ISSN: 19410476. DOI: 10.1109/TSP.2020.2995972.

[14] N. Tervo, B. Khan, O. Kursu, *et al.*, "Digital predistortion of phased-array transmitter with shared feedback and far-field calibration," *IEEE Transactions on Microwave Theory and Techniques*, vol. 69, no. 1, pp. 1000–1015, Jan. 2021, ISSN: 15579670. DOI: 10.1109/TMTT.2020.3038193.

[15] A. B. Ayed, Y. Cao, P. Mitran, and S. Boumaiza, "Digital predistortion of millimeter-wave arrays using near-field based transmitter observation receivers," *IEEE Transactions on Microwave Theory and Techniques*, vol. 70, no. 7, pp. 3713–3723, Jul. 2022, ISSN: 15579670. DOI: 10.1109/TMTT.2022.3174857.

[16] X. Wang, Y. Li, H. Yin, *et al.*, "Digital predistortion of 5G multiuser MIMO transmitters using low-dimensional feature-based model generation," *IEEE Transactions on Microwave Theory and Techniques*, vol. 70, no. 3, pp. 1509–1520, Mar. 2022, ISSN: 15579670. DOI: 10.1109/TMTT.2021.3129777.

[17] X. Wang, Y. Li, C. Yu, W. Hong, and A. Zhu, "OTA-based data acquisition and signal separation for digital predistortion of multi-user MIMO transmitters in 5G," in *IEEE MTT-S International Microwave Symposium Digest*, vol. 2020-August, IEEE, Aug. 2020, pp. 845–848, ISBN: 9781728168159. DOI: 10.1109/IMS30576.2020.9223978.

[18] K. Hausmair, U. Gustavsson, C. Fager, and T. Eriksson, "Modeling and linearization of multi-antenna transmitters using over-the-air measurements," in *Proceedings - IEEE International Symposium on Circuits and Systems*, vol. 2018-May, IEEE, Apr. 2018, ISBN: 9781538648810. DOI: 10.1109/ISCAS.2018.8351266.

[19] K. Hausmair, S. Gustafsson, C. Sanchez-Perez, *et al.*, "Prediction of nonlinear distortion in wideband active antenna arrays," *IEEE Transactions on Microwave Theory and Techniques*, vol. 65, no. 11, pp. 4550–4563, Nov. 2017, ISSN: 00189480. DOI: 10.1109/TMTT.2017.2699962.

[20] Q. Luo, X. W. Zhu, C. Yu, and W. Hong, "Single-receiver over-the-air digital predistortion for massive mimo transmitters with antenna crosstalk," *IEEE Transactions on Microwave Theory and Techniques*, vol. 68, no. 1, pp. 300–314, Jan. 2020, ISSN: 15579670. DOI: 10.1109/TMTT.2019.2943287.

[21] J. Fernandez, L. Anttila, M. Valkama, and T. Eriksson, "Linearization of active array transmitters under crosstalk via over-the-air observations," in *2023 31st European Signal Processing Conference (EUSIPCO)*, IEEE, 2023, pp. 1420–1424, ISBN: 9789464593600. DOI: 10.23919/EUSIPCO58844.2023.10289847.